Metal Oxide Thin Films Deposited from Metal Organic Precursors in Supercritical CO_2 Solutions

Theodosia Gougousi,*,† Dipak Barua, Erin D. Young,‡ and Gregory N. Parsons

Department of Chemical and Biomolecular Engineering, North Carolina State University, Raleigh, North Carolina 27695

Received May 23, 2005. Revised Manuscript Received July 29, 2005

This work demonstrates a novel method for deposition of metal oxide thin films, including Al_2O_3, ZrO_2, MnO_x, and RuO_x where the metal−organic precursors and oxidizing agents are delivered in liquid and supercritical CO_2. A cyclic deposition process is presented where reactants are introduced sequentially to control surface adsorption and byproduct removal steps. Reactions are studied in a hot wall reactor at pressures ranging from 1600 to 3600 psi at 80−200 °C, and X-ray photoelectron spectroscopy and infrared transmission confirmed metal oxide formation. We show that hydrogen peroxide is a viable O source for oxide deposition, whereas *tert*-butyl peracetate, which is a good electron acceptor, is less suited for oxygen donation. Capacitance versus voltage analysis of resulting Al_2O_3 films show good dielectric properties after post-deposition anneal. We believe that the good solvation properties of supercritical CO_2 can aid in the delivery of precursors and in the removal of byproducts for advanced low-temperature processing of oxides and other materials of interest in electronic applications.

Introduction

In most deposition and etching processes used for nanoelectronic device fabrication, kinetically controlled reactions such as reactant adsorption, surface oxidation (or reduction), and byproduct removal are driven by energy delivered to the surface via substrate heating or by other means including plasmas and photon or ion bombardment. These energy delivery approaches can damage the substrate or the deposited material itself. Another means to deliver energy is the use of solvation forces. These forces are not commonly applied in thin film processing, but they could be utilized to help enhance and expand the range of materials and conditions for thin film deposition and etching. Solvent-based processes, and in particular, supercritical fluid processes, are also attractive because they can deliver a high density of reactants to the surface while maintaining many of the beneficial aspects of gas-phase processes, including low viscosity and high diffusivity.[1] In principle, these properties of solvent-based processing could be used to promote specific desired reaction sequences. For example, additional energy provided by solvation forces could enable deposition of metals at very low temperatures on organic surfaces, where the solvent strength and structure is designed to remove the unwanted metal−organic ligand without affecting the molecular growth surface. Eventually, solvent-assisted deposition could provide a means to stabilize desired reaction intermediates during deposition to enable tuning of the structure and composition of the deposited film. Solution-based processes that involve solvation force effects are widely used for electroplating or autocatalytic (electroless) deposition[2,3] and other applications, but these approaches are generally not amenable to a wide range of materials.

The enhanced solvent characteristics of supercritical fluids[1] have been widely utilized for extraction, separation, polymerization,[4] and other chemical processes including metal thin film deposition.[5−7] The density of supercritical CO_2 (critical temperature 31 °C and critical pressure 7.4×10^6 Pa) can exceed that of liquids, but the diffusivity of species dissolved in CO_2 is between that of species in liquid ($\sim 10^{-5}$ cm^2/s) and gases (~ 1 cm^2/s) under typical process conditions. Supercritical CO_2 can suspend a significant density of molecular H_2, and the relatively high diffusivity can therefore enable a high flux of hydrogen or other soluble reactive species to be delivered to a deposition surface. For these studies, supercritical CO_2 was used because it is safe to handle and has an easily accessible supercritical point.[7,8]

Metal oxide materials are widely used in electronic devices for applications including high dielectric constant insulators in transistor structures,[9] magnetic tunnel junctions in spin-

* To whom correspondence should be addressed. E-mail: gougousi@umbc.edu.
† Current address: Dept. of Physics, University of Maryland Baltimore County, 1000 Hilltop Circle, Baltimore, MD 21250.
‡ Current address: Dept. of Chemical Engineering, University of Virginia, 102 Engineers' Way, P.O. Box 400741, Charlottesville, VA 22904-4741.

(1) McHugh, M.; Krukonis, V. J. *Supercritical Fluid Extraction*; Butterworth-Heinemann: Boston, 1994.
(2) Petrov, N.; Sverdlov, Y.; Shacham-Diamond, Y. *J. Electrochem. Soc.* **2002**, *149*, C187.
(3) Mallory, G. O.; Haydu, J. B. *Electroless Plating—Fundamentals and Applications*; American Electroplaters and Surface Finishers Society: Orlando, FL, 1990.
(4) DeSimone, J. M.; Maury, E. E.; Menceloglu, Y. Z.; McCain, J. B.; Romack, T. J.; Combes, J. R. *Science* **1994**, *265*, 356.
(5) Blackburn, J. M.; Long, D. P.; Cabanas, A.; Watkins, J. J. *Science* **2001**, *294*, 141.
(6) Long, D. P.; Blackburn, J. M.; Watkins, J. J. *Adv. Mater.* **2000**, *12*, 913.
(7) Watkins, J. J.; Blackburn, J. M.; McCarthy, T. J. *Chem. Mater.* **1999**, *11*, 213.
(8) Rathke, J. W.; Klinger, R. J.; Krause, T. R. *Organometallics* **1991**, *10*, 1350.
(9) Wilk, G. D.; Wallace, R. M.; Anthony, J. M. *J. Appl. Phys.* **2000**, *89* (10), 5243.

10.1021/cm0510965 CCC: $30.25
Published on Web 09/02/2005

tronic devices,[10] as well as for optical coatings, barrier layers, and catalytic materials. In this paper, we demonstrate preparation of metal oxide films from metal alkoxide precursors and oxidizing agents dissolved in liquid and supercritical carbon dioxide.

In most solvent-based thin film deposition processes, the substrate is exposed simultaneously to the precursor and oxidants (or reductants), leading to continuous growth, where the rate is determined by precursor supply or the rate of surface kinetic rate processes. An alternate approach, widely used in vapor-phase deposition, is to supply reactants sequentially, where adsorption and reaction steps are controlled individually. Atomic layer deposition, for example, involves sequential reactant exposure where each reaction step is self-limiting. In this paper, we demonstrate both continuous and time-sequenced chemical deposition of metal oxide films from precursors dissolved in liquid or supercritical CO_2.

Experimental Methods

The films were deposited on native oxide or H-terminated Si(100) surfaces. Both types of substrates were prepared by wet cleaning (JTB-100 Baker clean), deionized water rinse, and blown dry with N_2. For the H-terminated surfaces the dry substrates were dipped in buffered oxide etch (BOE) typically for 5−10 s until they appeared dewetted upon removal. Precursors for deposition included aluminum acetylacetonate (99%) ($Al(acac)_3$) [$Al(CH_3COCHCOCH_3)_3$], aluminum hexafluoroacetylacetonate (min. 98%) ($Al(hfac)_3$) [$Al(CF_3COCHCOCF_3)_3$], zirconium acetylacetonate (min. 98%) ($Zr(acac)_4$) [$Zr(CH_3COCHCOCH_3)_4$], tris(2,2,6,6-tetramethyl-3,5-heptanedionato)ruthenium(III), (99%, 99.9%-Ru) ($Ru(tmhd)_3$) [$Ru(C_{11}H_{19}O_2)_3$], and bis(cyclopentadienyl)ruthenium (99%, 99.9%-Ru) (ruthenocene) [$(C_5H_5)_2Ru$], purchased from Strem Chemicals. Manganese hexafluoroacetylacetonate trihydrate ($Mn(hfac)_2$) [$(C_4HF_6O)_2Mn\cdot 3H_2O$] was obtained from Sigma Aldrich. All precursors were used as received. The fluorinated precursors $Al(hfac)_3$ and $Mn(hfac)_2$ were stored in a well-sealed desiccator to prevent any reaction with moisture. Coleman-grade CO_2 with 99.99% purity was used for all the experiments.

All films were deposited in a home-made high-pressure ~20 mL stainless steel cell with sapphire windows. Pressurized CO_2 was delivered using an ISCO 260D syringe pump through a high-pressure manifold. Resistive heaters with feedback control were used to maintain the temperature of the reaction cell within ±1 °C of the set point value, and the lines used to deliver the precursor were typically heated to prevent precursor condensation. Two different deposition methods were explored: (1) batch processing, where all reactants were introduced to the deposition vessel simultaneously; and (2) cyclic processing, where reactants were introduced in a sequential repetitive manner to build films layer-by-layer. For batch processing, a piece of pretreated Si was placed inside the cell along with a known mass, usually 0.3−0.5 wt %, of the relevant precursor. The cell was then sealed, heated to 45 °C, and pressurized with CO_2 to the setpoint pressure. Then the temperature was raised to the desired reaction temperature, and the precursor was observed to dissolve. For some of the fluorinated metal organic precursors this was accomplished within a few minutes, and the dissolution could be monitored through the window. For less soluble precursors such as the acetylacetonates

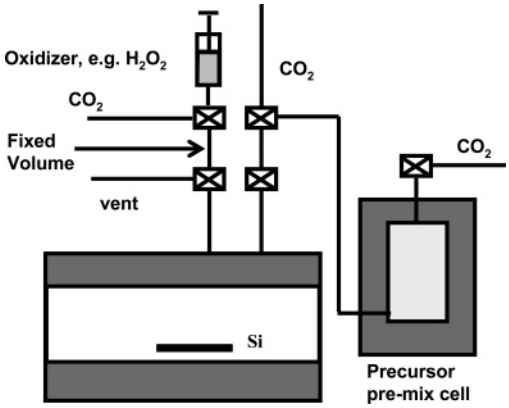

Figure 1. Schematic of the deposition system.

the precursors were allowed about 30 min to saturate the solution. To initiate film deposition, ~0.3 mL of the oxidizer solution was injected inside the high-pressure manifold and CO_2 from the syringe pump was used to push it into the cell. After a set reaction time (typically 30−90 min), the cell was purged with CO_2 and the effluent was filtered in an activated charcoal bed before venting. Two oxidizers were tested in the course of this work; a 30% aqueous solution of H_2O_2 and a 50% solution of *tert*-butyl peracetate ($CH_3CO_3C(CH_3)_3$) in mineral spirits. The H_2O_2 has very poor solubility in sc CO_2 while *tert*-butyl peracetate has very high solubility. In both cases, the oxidizer to precursor molar ratio was approximately 50, and the reagents were permitted to react for 30−90 min.

For the cyclic deposition process the substrate was exposed sequentially to the precursor and the oxidizer, as is commonly done in atomic layer deposition (ALD) processing. The experimental set up for this procedure is slightly different from that used in batch processing, and a schematic of the reactor system is shown in Figure 1. For these experiments, a larger high-pressure cell (~100 mL) was used as a precursor premix cell where the precursors were dissolved and held in supercritical carbon dioxide for subsequent use during the experiment. Before each experiment, the cleaned premix cell was flushed with CO_2 and loaded with approximately 20−30 mg of precursor. The premix cell was then pressurized with CO_2 at 1200−1500 psi and heated to 70−80 °C for 30 min before starting the deposition reaction. At the beginning of the process, the samples were loaded on the cleaned reaction cell, which was flushed with CO_2 at ~100 psi for 1 or 2 min, and then heated to 40−50 °C. The reaction cell was then pressurized above the critical pressure of CO_2 and heated to reach the set point temperature. After the temperature of the reaction cell equilibrated to the set point, the pressure inside the cell was adjusted to the setpoint value.

The experiments were carried out in ABAB cycles as in a typical atomic layer deposition process.[11] A small volume of precursor solution (A) at fixed pressure was transferred from the premix cell into a short tubing segment adjacent to the reactor cell, and this fixed volume of precursor solution was injected into the pressurized reaction cell, increasing pressure by 30−50 psi. After a set exposure time (30 s to 3 min), the reaction cell was flushed with a continuous stream of CO_2 to remove the remaining precursor, including any weakly adsorbed species on the deposition surface. The reaction cell was then re-pressurized with CO_2 and an oxidizing or a reducing agent (B), previously confined inside another fixed length of high-pressure tubing, was driven into the reaction cell with high-pressure CO_2 flow. The reactor was then flushed using a continuous CO_2 stream to avoid oxidizer precipitation on the substrate. For

(10) DeTeresa, J. M.; Barthelemy, A.; Fert, A.; Contour, J. P.; Montaigne, F.; Seneor, P. *Science* **1999**, *286*, 507.

(11) Ferguson, J. D.; Weimer, A. W.; George, S. M. *Chem. Mater.* **2000**, *12*, 3472.

aluminum oxide deposition, 0.2−0.4 mL of liquid oxidizer (30% aqueous solution of H_2O_2 or 50% *tert*-butyl peracetate in mineral spirits) was injected in each cycle. The duration of each cycle was approximately 15−20 min. Improved experimental approaches could enable shorter cycle times to be achieved.

The samples were characterized using X-ray photoelectron spectroscopy (XPS), transmission Fourier transform infrared spectroscopy (FTIR), and capacitance versus voltage measurements (*C*−*V*). The XPS measurements were performed with a Riber LAS3000 (MAC2 analyzer, Mg Kα $h\nu = 1253.6$ eV, nonmonochromatic X-ray source) at 75° takeoff-angle with 1 eV step size for survey scans, and 0.1 eV step size for high-resolution scans. We compensated for sample charge effects by setting the adventitious C 1s peak to a binding energy of 285.0 eV. A commercial software package (Casa XPS) was used to extract at. % film composition from the survey scans. The process related carbon content of the film is difficult to analyze by ex-situ XPS due to the adventitious carbon from the environment, and post-deposition carbonate formation due to reactions of the film with atmospheric CO_2. The fraction of bonded C reported below was roughly estimated from the total C film content and the relative intensity of the bonded and adventitious C 1s peaks in the high-resolution spectra. A ThermoNicolet IR bench equipped with a deuterated tri-glycine sulfate detector (KBr beam splitter) was used in the transmission mode, and for a typical spectrum we collect 256 scans at 4 or 8 cm^{-1} resolution. The instrument was purged using purified air with low concentrations of moisture and CO_2. A background spectrum was collected after each measurement using a substrate fragment that originated from the same wafer as the deposited substrate.

For electrical analysis aluminum top and back-contacts were formed by resistive-heating evaporation using shadow masks. Capacitance versus voltage measurements were performed with an HP 4284A impedance meter at 1 MHz. Typical capacitor area was $\sim 4.3 \times 10^{-4}$ cm^2. Flatband voltage (V_{fb}) and equivalent oxide thickness (EOT) were obtained by processing the *C*−*V* characteristics with the NCSU *C*−*V* program that includes corrections for the quantum mechanical effects.[12]

Results

Deposition of Al_2O_3 Films. *Batch Deposition Method.* Aluminum oxide films were deposited on Si substrates via both the batch and the cyclic deposition approach using aluminum acetylacetonate ($Al(acac)_3$) and its fluorinated equivalent, aluminum hexafluoroacetylacetonate ($Al(hfac)_3$), as precursors. Figure 2 shows high-resolution XPS scans of the Al 2p, C 1s, and O 1s regions for a film that was deposited using the batch approach on native oxide Si substrate at 120 °C and 1700 psi using $Al(acac)_3$ and H_2O_2. In the Al 2p region shown in Figure 2a, a broad feature located at 74.3 eV is observed. The width of the peak suggests that Al is present in the film in more than one oxidation state. The $2p_{3/2}$ electrons from elemental Al have a binding energy of 72.8 eV,[13] while $2p_{3/2}$ electrons from Al bound to O in Al_2O_3 have a binding energy of 74.6 eV.[14] The Al $2p_{3/2}$ electrons in AlO(OH) have a binding energy of 76.7 eV[15] and range[15,16] from 74.3 to 75.9 eV in $Al(OH)_3$. The high resolution scan for the O 1s region (Figure 2c)

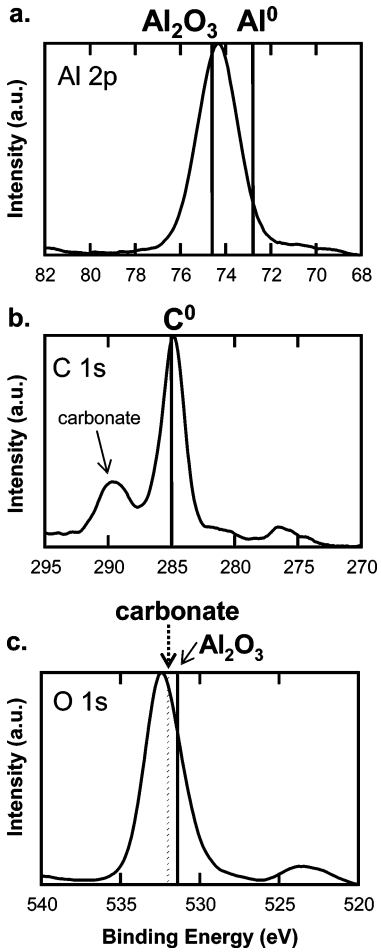

Figure 2. High-resolution scans for the (a) Al 2p, (b) C 1s, and (c) O 1s peaks for XPS survey scan for an Al-based film deposited from $Al(acac)_3$ and H_2O_2 at 120 °C and 1700 psi on Si substrates with native oxide. From the location and width of the peaks, we conclude that the film is a mixture of Al_2O_3, Al(OH)O, and aluminum carbonate.

shows a fairly broad peak at 532.4 eV, also consistent with a range of binding environments. The O 1s electron binding energy for Al_2O_3 is 531.4 eV,[17] which is similar to the O 1s binding energy for $Al(OH)_3$ at 531.53 eV[18] and that for AlO(OH) at 531.5.[16] The O 1s electrons in carbonate species are also known to have binding energies around ~532 eV.[19,20] The C 1s high-resolution scan shown on Figure 2b confirms the presence of bound carbon atoms in the film. Two peaks are clearly resolved; the one at 285 eV can be ascribed to adventitious C while the peak at 289.5 eV is indicative of C bonded to a more electronegative element, probably oxygen.

Transmission infrared spectroscopy can be used to confirm the presence of carbonate species in the film. Figure 3 (curve i) shows the infrared spectrum for an Al_2O_3 film prepared from $Al(acac)_3$ and H_2O_2 with conditions the same as for films in Figure 2. The 1200−1700 cm^{-1} spectral range is

(12) Yang, N.; Henson, K. W.; Hauser, J. R.; Wortman, J. J. *IEEE Trans. Electron Devices* **1999**, *46*, 1464.
(13) Domen, K.; Chuang, T. J. *J. Chem. Phys.* **1989**, *90*, 3318.
(14) Arata, K.; Hino, M. *Appl. Catal.* **1990**, *59*, 197.
(15) Lindsay, J. R.; Rose, H. J.; Swartz, W. E.; Watts, P. H.; Rayburn, K. A. *Appl. Spectrosc.* **1973**, *27*, 1.
(16) Taylor, J. A. *J. Vac. Sci. Technol.* **1982**, *20*, 751.
(17) Paparazzo, E. *Appl. Surf. Sci.* **1986**, *25*, 1.
(18) Wagner, C. D.; Passoja, D. E.; Hillery, H. F.; Kinisky, T. G.; Six, H. A.; Jansen, W. T.; Taylor, J. A. *J. Vac. Sci. Technol.* **1982**, *21*, 933.
(19) Bandoli, G.; Barreca, D.; Brescacin, E.; Rizzi, G. A.; Tondello, E. *Adv. Mater.: Chem. Vap. Dep.* **1996**, *2*, 238.
(20) Moulder, J. F.; Stickle, W. F.; Sobol, P. W.; Bomben, K. D. *Handbook of X-ray Photoelectron Spectroscopy*; Perkin-Elmer, Physical Electronics Division: Eden Prairie, MN, 1992.

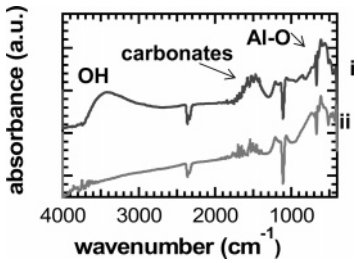

Figure 3. Transmission IR spectrum for an Al-based film deposited from $Al(acac)_3$ and H_2O_2 at 120 °C and 1700 psi on Si substrates with native oxide. Curve i shows a measurement taken after deposition, and curve ii shows a spectrum taken after the film was annealed at 600 °C in N_2 for 5 min. Spectrum i exhibits features at 1200−1700 cm^{-1} associated with several carbonate species. The broad peak at 3000−3600 cm^{-1} is due to the O−H stretching modes of both undissociated H_2O molecules and surface H-bonded OH species. Al−O bonding is detected by the broad peak at 400−800 cm^{-1}. Mild anneal results in the disappearance of the IR signature of the carbonates and hydroxides.

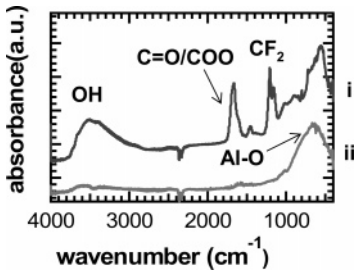

Figure 4. Transmission IR spectrum for an Al-based film deposited from $Al(hfac)_3$ and H_2O_2 at 130 °C and 2500 psi on Si substrates with the presence of H_2O in the film (3600−3000 cm^{-1}) and Al−O bonding (850−500 cm^{-1}). Well-resolved peaks at 1700 and 1300−1150 cm^{-1} are attributed to the presence of carbonate type and C−F bonding in the film. A mild anneal for 10 min at 600 °C in N_2 removes most of the IR signature of these impurities and reinforces the Al−O peak.

associated with absorptions from several carbonate species.[21] The broad peak at 3000−3600 cm^{-1} is due to the O−H stretching modes of both H_2O molecules and surface H-bonded OH species,[22] and the broad peak at 400−900 cm^{-1} indicates complex Al−O vibrations due to Al atoms in either tetrahedral or octahedral coordination surrounded by cubic close packing of oxygen atoms.[23]

On the basis of information from the XPS and the FTIR measurements, it is clear that the deposited film contains Al in a variety of bonding environments including oxide, carbonate (∼14 at. %), and hydroxide. A mild anneal of the film for 5 min in N_2 at 600 °C leads to desorption of the H_2O and carbonate species and enhancement of the Al−O peaks (Figure 3 curve ii). It is unclear whether the C-containing impurities are completely removed from the film, or if just the O species is desorbed leaving behind C in the bulk of the film.

Figure 4 shows the transmission IR spectrum for an Al_2O_3 film deposited from $Al(hfac)_3$ precursor with H_2O_2 as oxidizer at 130 °C and 2500 psi. The spectrum shows features corresponding to H_2O in the film (3600−3000 cm^{-1}) and Al−O bonding (850−500 cm^{-1}). Well-resolved peaks at

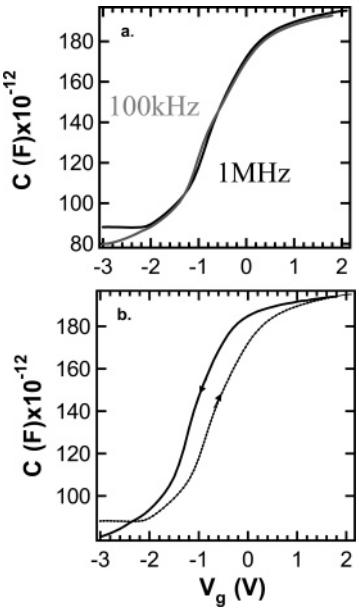

Figure 5. Frequency dependence (a) and hysteresis (b**)** of the *C* vs *V* measurements for Al-based film deposited from $Al(acac)_3$ and H_2O_2 at 80 °C, 2060 psi, and annealed at 600 °C in N_2 for 10 min. Change of frequency from 1 MHz to 100 kHz does not change the shape of the curve substantially, indicating good quality interface. However, the hysteresis at 1 MHz is quite large (∼500 mV).

1700 and 1300−1150 cm^{-1} are attributed to the presence of carbonate and C−F bonding in the film.[24] A mild anneal for 10 min at 600 °C in N_2 removes most of the IR signature of these impurities, strengthening the Al−O peaks. The results are consistent with O species desorbing, leaving behind some C and F in the bulk of the film.

The insulating properties of the Al_2O_3 films were evaluated by capacitance versus voltage measurements. Figure 5a shows the high (1 MHz) and low (100 kHz) frequency *C*−*V* curve for a film that was deposited from $Al(acac)_3$ and H_2O_2 at 80 °C and 2060 psi and was annealed at 600 °C in N_2 for 10 min. The *C*−*V* curves are similar at 1 MHz and 100 kHz, indicating the absence of substantial concentration of interface traps.[25] Based on the *C*−*V* data the equivalent oxide thickness (EOT) of the film is 71 Å, and the flatband voltage is ∼ −0.14 eV indicating the presence of a small amount of positive fixed charge. However, in Figure 5b the hysteresis for the 1 MHz curve for the same film is ∼500 mV indicating mobile charge in the bulk of the film.[25] This is likely due to charges associated with residual F contamination. Also, previous work on LaSiO films has shown that bulk carbonate and hydroxide species can form even after high-temperature anneals[26] possibly leading to additional charged defects.

Cyclic Deposition Method. Al_2O_3 films were also deposited with the cyclic process from $Al(acac)_3$ precursor with either H_2O_2 or *tert*-butyl peracetate solutions as oxidizers. Both oxidizers were used under similar temperature and pressure conditions, at 120 °C and 1600psi. For the H_2O_2 process, for 9 cycles a film thickness of ∼40 Å was measured using spectroscopic ellipsometry, while for the *tert*-butyl peracetate

(21) Busca, G.; Lorenzelli, V. *Mater. Chem.* **1982**, *7*, 89.
(22) Cerrato, G.; Bondiga, S.; Barbera, S.; Morterra, C. *Appl. Surf. Sci.* **1997**, *115*, 53.
(23) Madhu Kumar, P.; Balasubramanian, C.; Sali, N. D.; Bhoraskar, S. V.; Rohatgi, V. K.; Badrinarayanan, S. *Mater. Sci. Eng. B* **1999**, *63*, 215.
(24) Lau, K. K. S.; Caulfield, J. A.; Gleason, K. K. *Chem. Mater.* **2000**, *12*, 3032.
(25) Schroder, D. K. *Semiconductor Material and Device Characterization*, 2nd ed.; Wiley-Interscience, New York, 1998; p 338.
(26) Gougousi, T.; Parsons, G. N. *J. Appl. Phys.* **2004**, *95* (3), 1391.

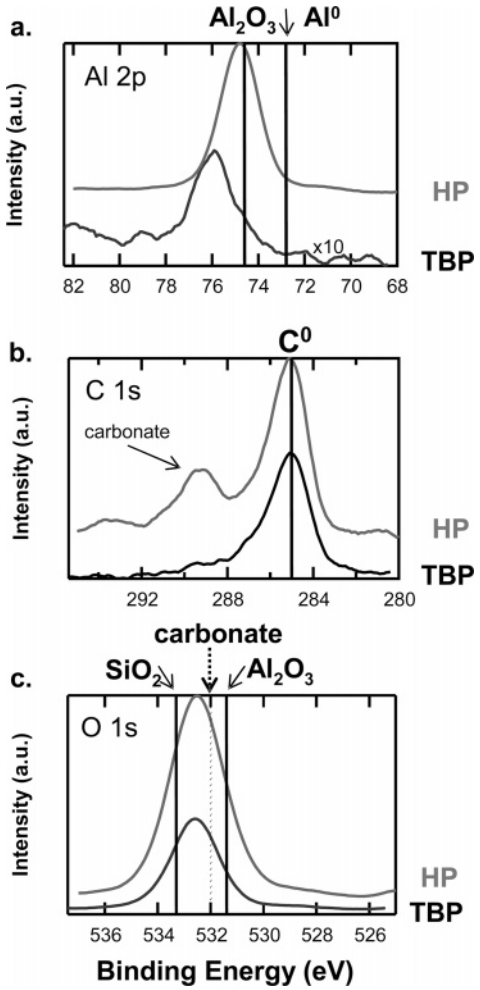

Figure 6. High-resolution XP scans for the (a) Al 2p, (b) C 1s, and (c) O 1s peaks for two Al-based films deposited via reagent cycling. Both films were deposited at 120 °C and 1600 psi. Film marked HP was deposited form $Al(acac)_3$ and H_2O_2, while film marked TBP was deposited from $Al(acac)_3$ and *tert*-butyl peracetate.

based process for 12 cycles, a film thickness of 35 Å was obtained. Thickness values from ellipsometry measurements were obtained assuming optical constants for Al_2O_3 on SiO_2. Figure 6 shows the high-resolution XP spectra for Al 2p C1s and O 1s core electrons for both films. The Al 2p spectrum (Figure 6a) is substantially different for the two samples. For the film deposited with hydrogen peroxide (labeled HP), a peak is observed at 74.8 eV indicative of Al−O bonds. For the film deposited using *tert*-butyl peracetate (labeled TBP) the peak is shifted to higher binding energy (∼75.5 eV), which indicates bonding of the Al atoms with more electronegative species. The C 1s spectrum shows the existence of adventitious C (peak at 285 eV) for both samples. For the HP sample, a second peak at 289.3 eV is well-resolved, evidence of carbonate formation in the film. For the TBP sample, the C 1s spectrum tails toward the higher binding energies with a shoulder at ∼289.5 eV. The O 1s spectra for both samples are quite similar containing contributions from SiO_2, Al_2O_3, hydroxides, and carbonates.

The relative intensity of the Al 2p peak (note the 10× multiplication factor for the *tert*-butyl peracetate sample) and the Si 2p peaks (not shown) indicate that the film deposited from HP is thicker that from TBP. On the basis of the binding energies of the O 1s electrons in Al_2O_3 (74.6 eV), AlO(OH) (76.7 eV), and $Al(OH)_3$ (74.3−75.9 eV), we conclude that the two films show evidence for hydroxides and carbonates. However, the proportion of these components in each film appears to be quite different. The location of the Al 2p peak indicates that (a) the film deposited using *tert*-butyl peracetate has a small Al_2O_3 content, most of the Al is bonded as AlO(OH) and some carbonate content (∼7 at. %), and (b) the film deposited using hydrogen peroxide has a higher Al_2O_3 and $Al(OH)_3$ content and some carbonate content (∼8 at. %). The higher OH content for the HP sample is likely related to the aqueous H_2O_2 solution used during the oxidation reaction. The process cycle for the TBP film does not include exposure to H_2O; however, aluminum oxides are hydrophilic and most likely the film absorbed H_2O from the ambient after removal from the high-pressure cell. It is not clear whether the carbonate formation occurs during the reaction or after ambient exposure. Other group III based oxides and silicates are very susceptible to reactions with atmospheric carbon dioxide to form various types of carbonate species.[26]

Batch Deposition of Other Metal Oxide Films. Several other metal organic precursors were tested using conditions similar to those used for batch deposition of Al_2O_3, and Table 1 gives a summary of all films deposited, including the precursor used and the oxidizing agent. Also included in the table are observations of general solubility of the precursors and whether film formation was observed. The following section describes XPS characterization data for some of these films.

Zr-Based Films. Figure 7 shows the Zr 3d, C 1s, and O 1s portions of the XP spectra for a Zr-based film that was deposited at 150 °C and 1700 psi using $Zr(acac)_4$ and *tert*-butyl peracetate as reagents. Detection of Si 2p photoelectrons from the Si substrate (data not shown) indicates the films are fairly thin (<50 Å). The Zr 3d peaks (Figure 7a) are clearly resolved at binding energies of 183 for the $3d_{5/2}$ and 185.3 eV for the $3d_{3/2}$ in good agreement with generally accepted binding energies for ZrO_2.[27] The two peaks are separated by 2.5 eV in good agreement with the 2.4 eV splitting reported.[27] The width of the peaks however suggests the presence of additional binding environments for the Zr atoms. For example, the binding energy of the Zr $3d_{5/2}$ electrons in the Zr−OH state is reported to be at 183.4 ∼0.5 eV higher than that in ZrO_2.[28] The width of the O 1s peak (Figure 7c), located at ∼532.5 eV, is also consistent with hydroxide in the films. The binding energy for the O 1s electrons in the Zr−OH state has been measured at 531.5 eV and that of Zr bound to H_2O at 533.3 eV.[20,29] Additionally, 1s electrons emanating from O in carbonate bonding have a binding energy of 532 eV. The C 1s high-resolution spectrum exhibits a peak at 589.5 eV, consistent with carbonate presence in the film. On the basis of the above

(27) Sinha, S.; Badrinarayanan, S.; Sinha, A. P. B. *J. Less-Common Metals* **1986**, *125*, 85.
(28) Li, Y. S.; Wang, P. C.; Mitchell, K. A. R. *Appl. Surf. Sci.* **1995**, *89*, 263.
(29) Basu, B.; Vitchev, R. G.; Vleugels, J.; Celis, J. P.; Van Der Biest, O. *Key Eng. Mater.* **2002**, *206−213*, 783.

Table 1. Summary of All Films Deposited Using the Supercritical Carbon Dioxide Technique[a]

material	precursor	solubility	oxidizer	method	T (°C)	comments
Al_2O_3	$Al(acac)_3$	poor	30% H_2O_2 in H_2O	batch	70−120	thick films
			50% *tert*-butyl peracetate in mineral spirits	batch	120	thinner films, precipitates
			oxygen	batch	120	no visible film
	$Al(acac)_3$	poor	30% H_2O_2 in H_2O	cyclic	120	multilayer growth per cycle
			50% *tert*-butyl peracetate in mineral spirits	cyclic	120	thinner growth per cycle
	$Al(hfac)_3$	very good	30% H_2O_2 in H_2O	batch	80−120	thick films, with fluorine
			50% *tert*-butyl peracetate in mineral spirits	batch	150	thin films, with fluorine
ZrO_2	$Zr(acac)_4$	poor	30% H_2O_2 in H_2O	batch	120−200	thin film
			50% *tert*-butyl peracetate in mineral spirits	batch	150	thin film
HfO_2	$Hf(acac)_4$	poor	30% H_2O_2 in H_2O	batch	120−200	not characterized
	TDEAHf	precursor oxidized	30% H_2O_2 in H_2O	batch	100−150	precipitates
ZnO_x	$Zn(hfac)_4$	very good	30% H_2O_2 in H_2O	batch	150	not characterized
MnO_x	$Mn(hfac)_2$	very good	30% H_2O_2 in H_2O	batch	100−150	thin film, with fluorine
RuO_x	$Ru(tmhd)_3$	good	30% H_2O_2 in H_2O	batch	100−150	thin film
			50% *tert*-butyl peracetate in mineral spirits	batch	100−120	thin film
	$Ru\ Cp_2$	poor	30% H_2O_2 in H_2O	batch	90−180	thin film
Y_2O_3	$Y(tmhd)_3$	good	30% H_2O_2 in H_2O	batch	120−150	thick film, carbon contamination

[a] Information on precursors used and oxidizing agents and observations of general solubility of the precursors and film formation are included.

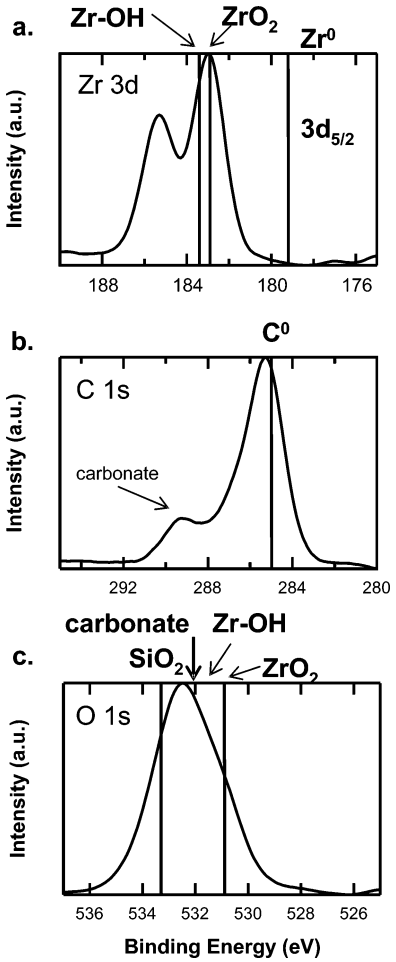

Figure 7. High-resolution XP scans for the (a) Zr 3d, (b) C 1s, and (c) O 1s peaks for a Zr-based film deposited from $Zr(acac)_4$ and *tert*-butyl peracetate at 150 °C and 1700 psi. The film composition can best be described as hydroxycarbonate.

observations, we can conclude that the Zr-based film contains ZrO_2, Zr−OH, and a substantial fraction of zirconium carbonate (∼15 at. %).

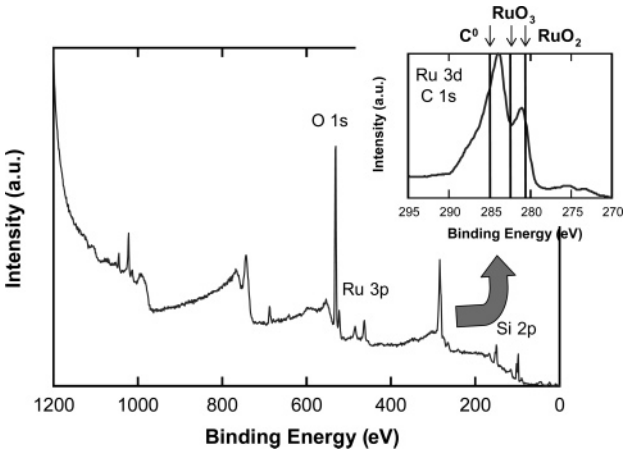

Figure 8. XP survey spectrum for a Ru-based film deposited from $Ru(tmhd)_3$ and H_2O_2 at 150 °C and 3600 psi. The presence of the Ru 3d and Ru 3p peaks verify the deposition of a Ru-based film on Si substrate. The insert graph shows a high-resolution scan of the Ru 3d/C 1s region.

Ru-Based Films. Figure 8 shows the survey spectrum for a Ru-based film deposited from $Ru(tmhd)_3$ and H_2O_2 at 150 °C and 3600 psi. In this spectrum Ru 3p and Ru 3d peaks are clearly visible, along with the O 1s, C 1s, and Si 2p peaks. The Ru 3d peaks overlap partially with the C 1s peak, and a high-resolution scan of this range is shown in the insert. In this spectrum, peaks at 281.1 and 284 eV with a large high-binding energy tail are resolved clearly. Because the lowest binding energy for C 1s core electrons is 285 eV for adventitious carbon, the peak at ∼281.1 eV is assigned to the Ru $3d_{5/2}$ component. The existence of the Ru 3p peaks in the survey spectrum corroborates the presence of Ru in the film and this peak assignment. Ru can form several oxides that vary in the binding energy of the Ru 3d peaks. For RuO_2 the $3d_{5/2}$ electrons appear at 280.6 eV[30] while the ones from RuO_3 are at 282.5 eV.[31] The location of the

(30) Sarma, D. D.; Rao, C. N. R. *J. Electron Spectrosc. Relat. Phenom.* **1980**, *20*, 25.

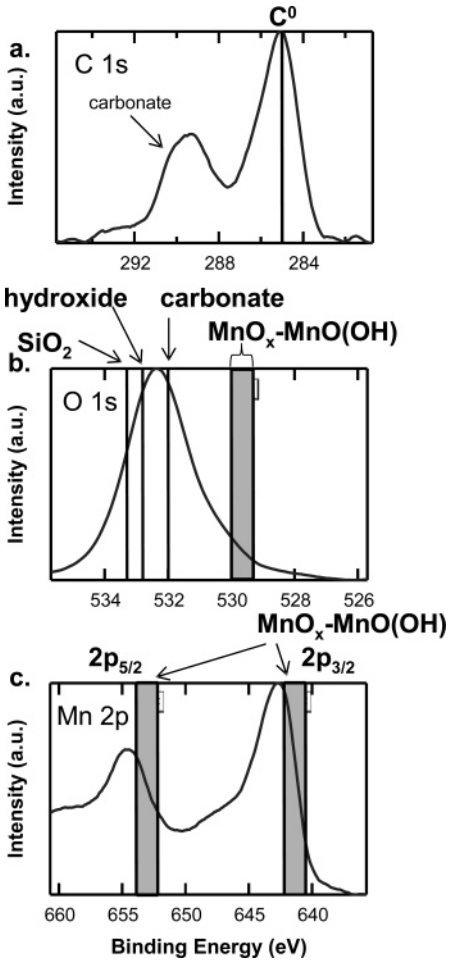

Figure 9. High-resolution XP scans for the (a) C 1s, (b) O 1s, and (c) Mn 2p peaks for a Mn-based film deposited from $Mn(hfac)_2$ and H_2O_2 at 150 °C and 3500 psi. The highlighted area on plots b and c show the range of binding energies available to O 1s and M 2p electrons due to the large number of oxidation states available to the Mn atoms. The film contains a mixture of manganese oxides, carbonates, and hydroxides.

observed peak at 281.1 eV may indicate the existence of both RuO_2 and RuO_3 in the film. The O 1s spectrum (not shown) confirms the presence of multiple Ru oxidation states in the film. The high-binding energy tale of the 284.1 eV peak may indicate the presence of Ru−OH and/or ruthenium carbonate species as well. The carbonate content of the film was not determined due to the overlap of the C 1s with the Ru 3d peaks. RuO_x deposition was also achieved by using bis(cyclopentadienyl) ruthenium (ruthenocene) and H_2O_2 at 130 °C and 3120 psi. The XP survey and Ru 3d spectra are very similar to those obtained from $Ru(tmhd)_3$ and H_2O_2.

Mn-Based Films. Figure 9 presents high-resolution spectra for C 1s, O 1s, and Mn 2p for a Mn-based film, deposited from $Mn(hfac)_2$ and H_2O_2 at 150 °C and 3500 psi. The XP survey scan (not shown) exhibits well-resolved peaks for F 1s (F ∼5 at. %) and Si 2p electrons, and the intensity of the Si 2p photoelectrons is consistent with a thin film (<50 Å). For the Mn 2p peaks, the $2p_{3/2}$ and $2p_{5/2}$ are located at 653.9 and 642 eV and show a splitting of 11.9 eV in good agreement with the 11.7 eV generally cited.[32] Mn appears in oxides with a variety of oxidation states and the 2p core electrons reflect that difference in the binding energy. For the $2p_{5/2}$ component, reported binding energies range from 640.5 eV for MnO[33] to 642.2 eV for MnO_2.[34] Other Mn-based oxides are Mn_2O_3 with a binding energy of 642 eV[32] and Mn_3O_4 with a binding energy of 641.2.[33] Finally, Mn bound in MnO(OH) has a binding energy of 641.7 eV.[33] Figure 9c shows shaded regions corresponding to these manganese oxide peaks, and these are referred to here as MnO_x. Since the Mn peaks in Figure 9c occupy a more extended region than the MnO_x highlighted area, we conclude that Mn is bound to O in other configurations and/or bound to other elements. The C 1s and O 1s spectra are also consistent with a variety of binding states for the Mn in the films. The C 1s spectrum in Figure 9a shows a peak at 288.8 eV indicative of carbonate bonding, and the O 1s peak in Figure 9b is broad with a peak at 532.7 eV. The peak is shifted from the expected MnO_x peak position near 530 eV, consistent with carbonate and hydroxide in the film.[19,35]

Discussion and Summary

This work demonstrates that a variety of metal oxides films can be deposited using precursors soluble in supercritical carbon dioxide and that the extent of oxidation depends on the nature of the oxidizing species. Hydrogen peroxide and *tert*-butyl peracetate were used as oxidizers, and the aqueous peroxide solution was generally more successful for achieving oxide film growth, even though it is generally less soluble than the *tert*-butyl peracetate in sc CO_2. Even at low solubility, a sufficient concentration of the peroxide in sc CO_2 can be delivered to the growth surface for metal and ligand oxidation. The solvation energy related to the solubility of the oxidized ligands may provide additional driving force, along with the mild thermal energy, for ligand removal and film growth. However, when aqueous hydrogen peroxide is used as the oxygen source significant H_2O is observed in the metal oxide film as confirmed by infrared and XPS data. Nonaqueous *tert*-butyl peracetate has been used in etching of Cu(0) in sc CO_2,[36,37] and it is highly soluble in sc carbon dioxide. In the oxide deposition reaction, the oxidation state of the metal atom (i.e., Al^{3+}) is the same in the precursor and in the final oxide film, and oxygen donation is not necessarily required to complete the reaction. However, in this case, breaking a strong C═O bond is required to produce the metal oxide film, and a reactant readily able to donate oxygen atoms would be more preferable. While the TBA can readily act as an oxidizing agent and accept electrons, it is less likely to provide oxygen for the reaction or break the C═O bond; therefore, film growth does not readily proceed, leaving carbon and other precursor byproducts on the surface

(31) Kim, K. S.; Winograd, N. *J. Catal.* **1974**, *35*, 66.
(32) Tan, B. J.; Klabunde, K. J.; Sherwood, P. M. A. *J. Am. Chem. Soc.* **1991**, *113*, 855.
(33) Oku, M.; Hirokawa, K. J. *Electron Spectrosc. Relat. Phenom.* **1976**, *8*, 475.
(34) Allen, G. C.; Harris, S. J.; Jutson, J. A.; Dyke, J. M. *Appl. Surf. Sci.* **1989**, *37*, 111.
(35) Martensson, N.; Malmquist, P. A.; Svensson, S.; Basilier, E.; Pireaux, J. J.; Gelius, U.; Siegbahn, K. *Nouveau J. Chim.* **1977**, *1*, 191.
(36) Bessel, C. A.; Denison, G. M.; DeSimone, J. M.; DeYoung, J.; Gross, S.; Schauer, C. K.; Visintin, P. M. *J.* Am. Chem. Soc. **2003**, *125*, 4980.
(37) Visintin, P. M.; Bessel, C. A.; White, P. S.; Schauer, C. K.; DeSimone, J. M. *Inorg. Chem.* **2005**, *44*, 316.

due to incomplete oxidation. This is consistent with ellipsometry data that shows lower Al_2O_3 film thickness for films deposited with TBP as compared to H_2O_2. It is also consistent with IR and XPS results for Al_2O_3 and ZrO_2 that show more carbonate and hydroxide contents in films deposited from TBP as compared to H_2O_2. Other nonaqueous oxidizers could be of interest, especially for applications involving the hygroscopic group III metal oxides.

In this work, we also explored cyclic processing of oxide thin films in sc CO_2, where the precursor and oxidizer are introduced sequentially. The cyclic process will eliminate possible homogeneous reactions between reactants, and it would enhance the ability of the solution to remove reaction byproducts from the surface during processing, leading to improved oxide materials with lower impurity concentrations. XPS results for Al_2O_3 films deposited using $Al(acac)_3$ and H_2O_2 using the batch and cyclic process are shown in Figures 2 and 6, respectively. Both films exhibit strong carbonate peaks, but further analysis of the data shows that the carbon content of the ALD film is smaller as compared to the batch-processed film. The ALD film shows evidence for residual contamination of fluorine, so careful cleaning of the cell between experiments is required to avoid cross contamination. We note that the growth thickness per deposition cycle for the Al_2O_3 films deposited from $Al(acac)_3$ and H_2O_2 ranges from ~2 to 8 Å per cycle,[38] which is larger than the typical monolayer or submonolayer per cycle observed in typical ALD processes, consistent with multiple monolayers of growth per cycle. This multilayer growth may limit reaction byproduct desorption, and we believe that processing with alternate precursors with better propensity for self-limiting adsorption will result in reduced impurities and better quality films.

Watkins and co-workers have shown that Cu, Ni, Pt, Pd, Au, and Rh metal films can be deposited by CFD with fairly low impurity contents.[5,6] For example, Cu metals films with <0.1 at. % C and <0.1 at. % F were formed at 250 °C.[5] The XPS results presented here cannot be used to separate the process-related carbonate content from that due to post-deposition reaction with atmospheric CO_2 which is quite common for metal oxides.[21,22,26] However, based on the size of the carbonate and fluorine peaks in the XPS data, we conclude that the bonded carbon in our films from both sources can be several atomic percent. The film F content varies from <1% to several atomic percent depending on the precursor and, more significantly, on the history of the cell (residual contamination). Both impurities are higher than the best results reported for metals deposition by CFD. This difference may result because, in general, carbonate bonding is less favored in the noble metals as compared to the metal oxides and because the processes reported here were not optimized to minimize carbon and other impurity content. Further efforts in sc CO_2 processing may likely lead to metal oxides with improved impurity.

This work has demonstrated that a variety of metal oxide films can be deposited at low temperature from precursors dissolved in supercritical solvents and that the extent and rate of the deposition reaction depends on the precursor and oxidizing species used. A novel cyclic deposition process has been demonstrated where reactants are introduced sequentially to control homogeneous reactions and control surface adsorption and byproduct removal steps. Hydrogen peroxide is a viable source of oxygen for oxide deposition, whereas *tert*-butyl peracetate, which is a good electron acceptor, is less suited for oxygen donation in the deposition reaction. We believe that the good solvation properties of sc CO_2 can aid in the delivery of precursors and in the removal of byproducts for advanced low-temperature processing of oxides and other materials of interest in electronic applications.

Acknowledgment. Financial support from NSF (Grant CTS-0304296) and the NSF Science and Technology Center for Environmentally Responsible Solvents and Processes is gratefully acknowledged. We also acknowledge Dr. Ke Wang for assistance with the sc CO_2 experimental setup and Prof. Ruben Carbonell for helpful discussions.

CM0510965

(38) Barua, D. M.S. Thesis, North Carolina State University, Raleigh, 2005.